

AWARD NUMBER: W81XWH-15-1-0056

TITLE: Do Prostate Cancer Exosomes Generate a Field Effect leading to Tumor Multifocality?

PRINCIPAL INVESTIGATOR: Marco Bisoffi, PhD

CONTRACTING ORGANIZATION: Chapman University
Orange CA 92866

REPORT DATE: June 2018

TYPE OF REPORT: Final

PREPARED FOR: U.S. Army Medical Research and Materiel Command
Fort Detrick, Maryland 21702-5012

DISTRIBUTION STATEMENT: Approved for Public Release;
Distribution Unlimited

The views, opinions and/or findings contained in this report are those of the author(s) and should not be construed as an official Department of the Army position, policy or decision unless so designated by other documentation.

REPORT DOCUMENTATION PAGE

Form Approved
OMB No. 0704-0188

Public reporting burden for this collection of information is estimated to average 1 hour per response, including the time for reviewing instructions, searching existing data sources, gathering and maintaining the data needed, and completing and reviewing this collection of information. Send comments regarding this burden estimate or any other aspect of this collection of information, including suggestions for reducing this burden to Department of Defense, Washington Headquarters Services, Directorate for Information Operations and Reports (0704-0188), 1215 Jefferson Davis Highway, Suite 1204, Arlington, VA 22202-4302. Respondents should be aware that notwithstanding any other provision of law, no person shall be subject to any penalty for failing to comply with a collection of information if it does not display a currently valid OMB control number. **PLEASE DO NOT RETURN YOUR FORM TO THE ABOVE ADDRESS.**

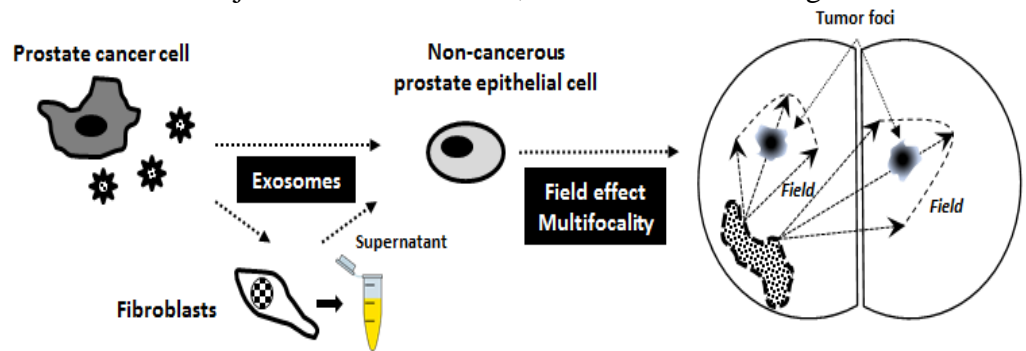
1. REPORT DATE June 2018		2. REPORT TYPE Final		3. DATES COVERED 03/25/2015 to 03/24/2018	
4. TITLE AND SUBTITLE Do Prostate Cancer Exosomes Generate a Field Effect leading to Tumor Multifocality?				5a. CONTRACT NUMBER	
				5b. GRANT NUMBER W81XWH-15-1-0056	
				5c. PROGRAM ELEMENT NUMBER	
6. AUTHOR(S) Marco Bisoffi bisoffi@chapman.edu				5d. PROJECT NUMBER 0010631947	
				5e. TASK NUMBER	
				5f. WORK UNIT NUMBER	
7. PERFORMING ORGANIZATION NAME(S) AND ADDRESS(ES) Chapman University, Schmid College of Science and Technology, One University Drive, Orange, California 92626				8. PERFORMING ORGANIZATION REPORT NUMBER	
9. SPONSORING / MONITORING AGENCY NAME(S) AND ADDRESS(ES) U.S. Army Medical Research and Materiel Command Fort Detrick, Maryland 21702-5012				10. SPONSOR/MONITOR'S ACRONYM(S)	
				11. SPONSOR/MONITOR'S REPORT NUMBER(S)	
12. DISTRIBUTION / AVAILABILITY STATEMENT Approved for Public Release; Distribution Unlimited					
13. SUPPLEMENTARY NOTES None					
14. ABSTRACT Prostate field effect (or field cancerization) denotes the presence of molecular aberrations featured in structurally intact cells of histologically normal tissues adjacent to adenocarcinomas, in many cases as distant as centimeters from the tumor margin. The presence of a field effect is causatively associated with the occurrence of tumor multifocality in the prostate, but a notable gap of knowledge is the lack of understanding of how multifocal fields of molecular aberrations in histologically normal tissues adjacent to tumors form. In this project, we have proposed a novel line of investigation that hypothesizes the implication of tumor-derived exosomes in the formation of field effect and tumor multifocality. Exosomes are extracellular microvesicles secreted by cells for the purpose of inter-cell and inter-tissue communication. Their biological function lends itself for a potential involvement in the formation of pre-malignant fields, especially when they are secreted by pre-existing cancer cells into neighboring tissues with histologically normal architecture. We pursued two Specific Aims to test our hypothesis: (i) To test the cellular and molecular effect of prostate cancer exosomes on non-cancerous cells, and (ii) to determine the association between markers of field effect and markers of exosomes in tissues adjacent to adenocarcinomas. Support from the DOD for this project has allowed us to: (i) Establish the isolation and biochemical characterization of exosomes from prostate cells cancer; (ii) determine the effects of tumor-derived exosomes on normal prostate epithelial cells; (iii) determine the correlation between a marker of exosomes (CD9) and at least one marker of field effect (EGR-1); (iv) complete a manuscript and publish it, as well as prepare a second manuscript which is close to submission; and (v) build strategically meaningful alliances with researchers at neighboring institutions. We propose a distinctive clinical importance for the involvement of exosomes in the etiology of prostate field effect, both related to the clinical management of prostate cancer patients in the pre-surgical setting and relating to biopsies: Exosomal markers, as well as markers of field effect, enlarge the clinically informative area of a biopsy, which could lead to the reduction of false negative detection rates in first biopsies procured with diagnostic intent for men with suspected prostate cancer, and/or in repeat biopsies procured from men with confirmed prostate cancer who chose active surveillance with frequent monitoring. We envisage the following next steps: (i) To extend our findings to tissues featuring multifocal tumors and test a possible correlation between exosomal and field effect markers with the extent of tumor multifocality; (ii) to determine the genomic and proteomic effects of tumor exosomes on normal prostate epithelial and stromal cells for the identification of additional markers; (iii) to functionally recapitulate the formation of a field effect by cancer exosomes in animal models of prostate cancer; and finally (iv) to test the validity of exosomal and field effect markers in active/prospective cohorts of patients enrolled in active surveillance.					
15. SUBJECT TERMS					
16. SECURITY CLASSIFICATION OF:			17. LIMITATION OF ABSTRACT Unclassified	18. NUMBER OF PAGES 22	19a. NAME OF RESPONSIBLE PERSON USAMRMC
a. REPORT Unclassified	b. ABSTRACT Unclassified	c. THIS PAGE Unclassified			19b. TELEPHONE NUMBER (include area code)

Table of Contents

	<u>Page</u>
1. Introduction.....	4
2. Keywords.....	4
3. Accomplishments.....	4-8
4. Impact.....	8-9
5. Changes/Problems.....	9
6. Products.....	9
7. Participants & Other Collaborating Organizations.....	10
8. Special Reporting Requirements.....	10
9. Appendices.....	10

1. Introduction

Prostate field effect (or field cancerization) denotes the presence of molecular aberrations featured in structurally intact cells of histologically normal tissues adjacent to adenocarcinomas, in many cases as distant as centimeters from the tumor margin. Prostate field effect is increasingly accepted as a type of molecular pathology with potentially far-reaching clinical implications (see Impact below). The presence of a field effect is causatively associated with the occurrence of tumor multifocality in the prostate, but a notable gap of knowledge is the lack of understanding of how multifocal fields of molecular aberrations in histologically normal tissues adjacent to tumors form. We propose a novel line of investigation by combining for the first time the concept of field effect with the concept of exosome trafficking. Exosomes are a type of extracellular nanovesicles that are secreted by prostate epithelial cells, and that carry a multitude of factors that affect cellular physiology. In grant W81XWH-15-1-0056e we hypothesize a novel and as yet unexplored role of prostate cancer exosomes, namely that they are “messengers” of field formation in histologically normal tissues adjacent to adenocarcinomas, and that their “cargo” primes areas outside of the tumor margin for additional tumor development (figure). This venue has not been previously pursued and represents an entirely new line of questioning. The rationale for this is based on the premise that exosomes carry factors that can alter the physiology of cells and tissues at greater distances. By extension, they could induce markers and mediators of tumorigenesis in histologically normal tissues adjacent to solid tumors, or a field effect. In agreement with the scope of an Exploration - Hypothesis Development Award, the objective is to test our hypothesis for the generation of preliminary data that will justify more translational follow-up studies with preclinical character.



Specific Aim 1: To test the effect of prostate cancer exosomes on non-cancerous cells. The specific tasks of Aim 1 are to determine whether prostate cancer exosomes induce markers characteristic of field effect and whether such activation induces elevated proliferation and/or reduced apoptosis.

Specific Aim 2: To determine the association between markers of field effect and markers of exosomes in tissues adjacent to adenocarcinomas. The specific tasks of Aim 2 are to determine whether the presence and expression level of markers of field effect and markers of exosomes correlate in tumor adjacent tissues; and to assess whether these parameters differ in adjacent tissues derived from unifocal vs. multifocal prostate cancers.

2. Keywords

Prostate cancer, tumor multifocality, field effect, pre-malignancy, biopsies, exosomes, CD9, early growth response 1 (EGR-1), fatty acid synthase (FASN)

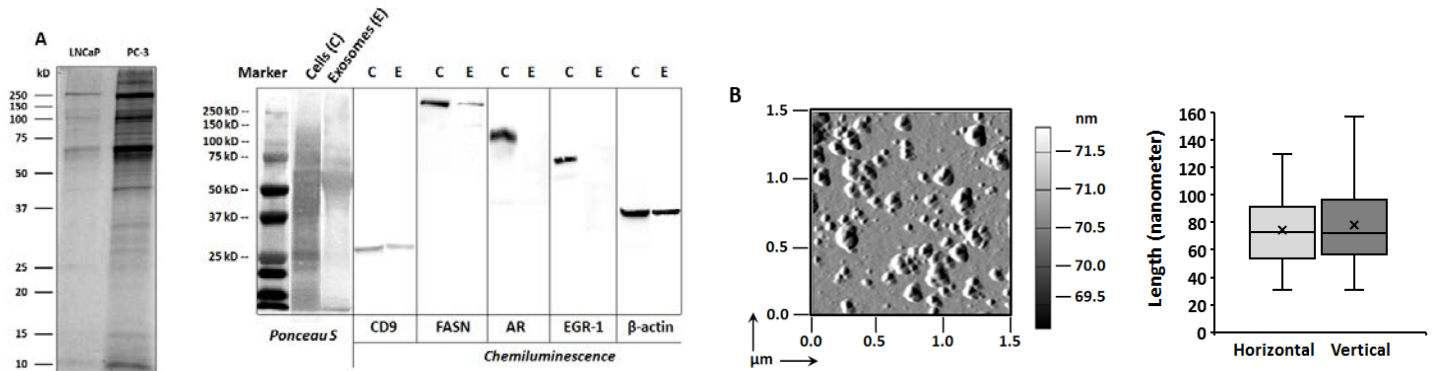
3. Accomplishments

What were the major goals of the project? What was accomplished under these goals?

Per the Statement of Work, the major goal of Specific Aim 1 was to test the effect of prostate cancer exosomes on non-cancerous prostate cells, and the major goal of Specific Aim 2 was to determine the association between markers of field effect and markers of exosomes in tissues adjacent to adenocarcinomas. Given the fact that a second publication is in preparation (see below), the scope of Aim 1 was achieved to approximately 75%, while the scope of Aim 2 was achieved to approximately 90%. Selective and essential experimental data pertinent to the goals of both Specific Aims 1 and 2 are shown below:

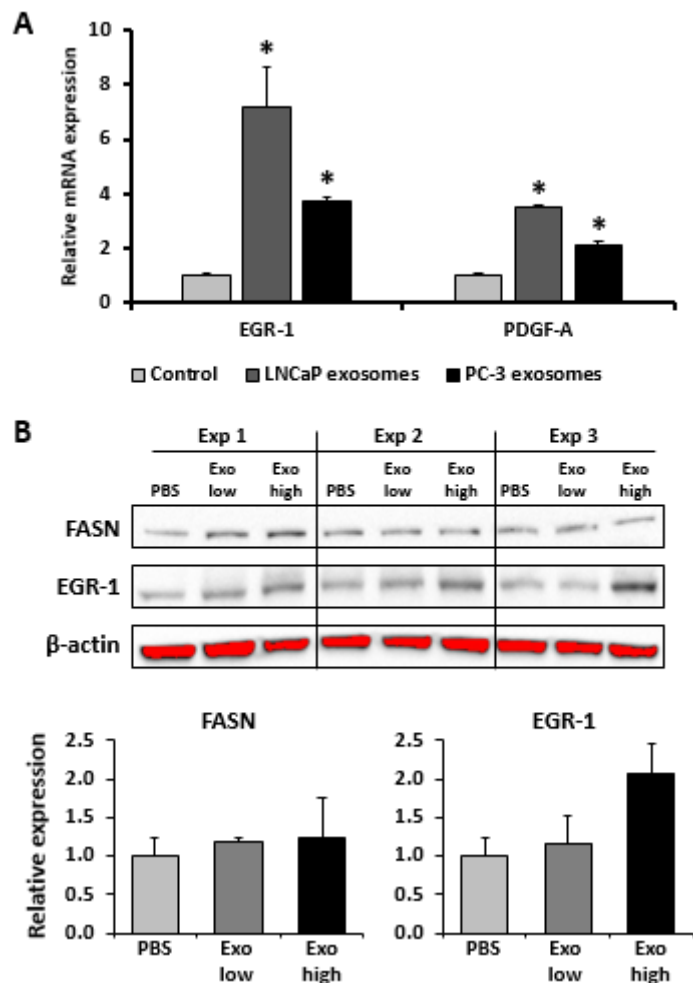
Isolation and partial characterization of exosomes from prostate cells

We have established an ultracentrifugation based protocol for the isolation of exosomes from a variety of human prostate cell models, including the non-cancerous RWPE-1 and the cancerous LNCaP and PC-3 cells. The figures below show their biochemical and physical characterization: (A) Protein profiles, as revealed by sodium dodecyl sulfate polyacrylamide gel electrophoresis (SDS-PAGE) (left) and Western blot analysis for exosomal markers in LNCaP exosomes (right). (B) Visualization of LNCaP exosomes by light scattering (left) and their quantitative horizontal and vertical measurements (right).



Effect of prostate cancer cell exosomes on markers of field effect in normal cells

We have explored the effect of exosomes released from prostate cancer cells (LNCaP and PC-3) on the cells of the non-cancerous phenotype (RWPE-1). In particular, we are interested in determining whether such exosomes can induce established markers of field effect, including the ones that we have reported previously, such as early growth response 1 (EGR-1), platelet derived growth factor A (PDGF-A), and fatty acid synthase (FASN). The figure to the right shows the effect of LNCaP and PC-3 released exosomes on the mRNA expression of EGR-1 and PDGF-A in the non-cancerous prostate epithelial cells RWPE-1 (A). At the protein level, LNCaP prostate cancer cell derived exosomes induced the expression of EGR-1, but not FASN in RWPE-1 in three independent experiments (B). While there is variation, this data indicates that exosomes released from prostate cancer cells induce markers of field effect in normal cells, which is in support of our main hypothesis.



Association between markers of exosomes and markers of field effect in human prostate tissues

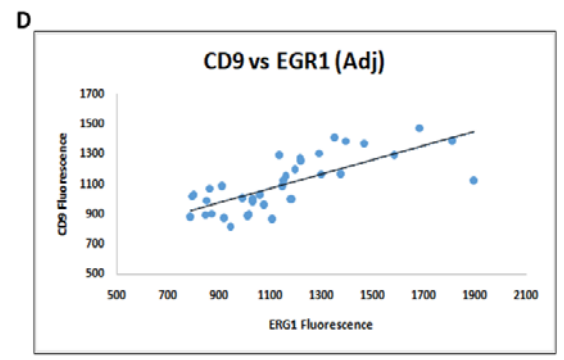
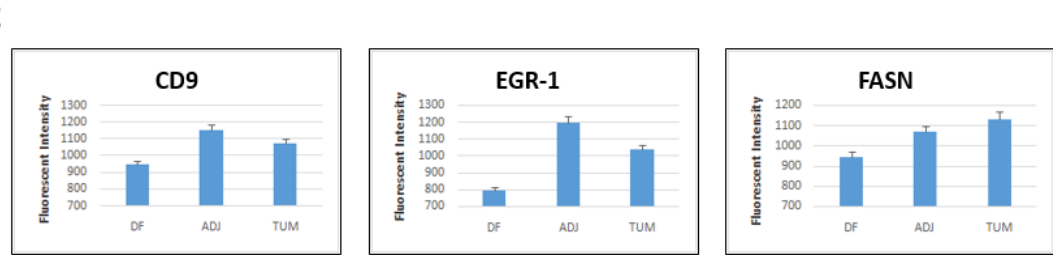
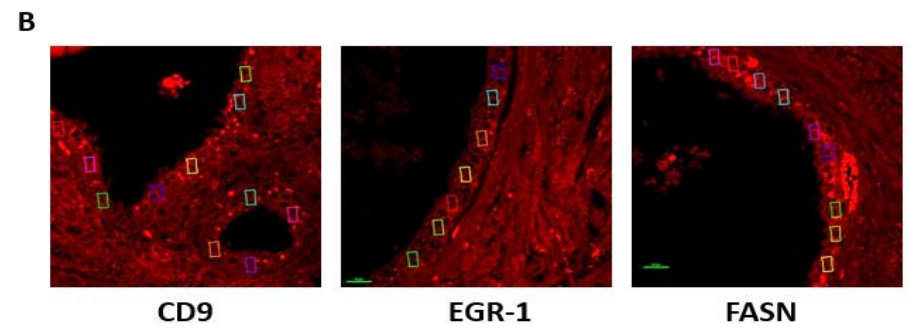
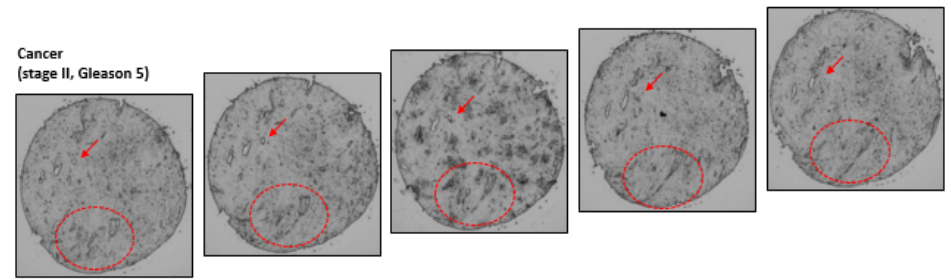
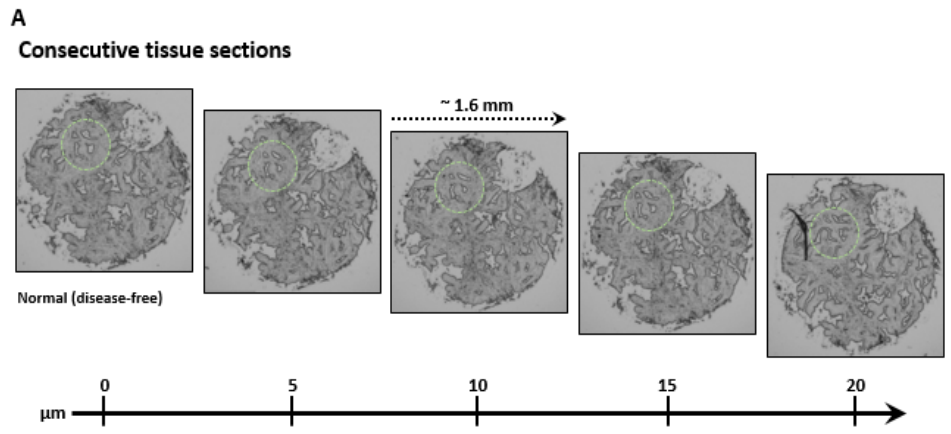
The data above prompted us to test the hypothesis that exosomal markers, such as CD9, are associated with markers of field effect, such as EGR-1 and potentially, FASN, in human tissues resected from histologically overt cancers, histologically normal tissue areas adjacent to adenocarcinomas (field cancerized), and disease-free (cancer-unrelated) prostatic tissues. This was the major task of Specific Aim 2. To test this hypothesis, we utilized commercially available tissue microarrays featuring slides with consecutive sections, as shown in the figure below (A).

We used specific antibodies in quantitative immunofluorescence to determine the expression level of the exosomal marker CD9 and the markers of field effect/cancerization EGR-1 and FASN. Due to the well-known heterogeneity of expression of any protein in human tissue samples, we determined expression the of these markers in different areas of the specimens by placing multiple regions of interest (ROI) on the digitized images of the all cases analyzed. Representative images of this procedure are shown in the figure below (B), where the ROI are shown as colored rectangles.

Quantification of the fluorescence signals (representative of expression levels) revealed the following: EGR-1 and FASN were confirmed to exert a field effect in this independent tissue cohort, as shown in figure C. In addition, we can report the new finding that the expression of the exosomal marker CD9 was similar in cancerous and histologically normal tissues adjacent to tumors, and upregulated when compared to disease-free tissues. CD9 could thus be an additional marker of field effect.

The most pertinent finding was the positive correlation between the exosomal marker CD9 and the marker of field effect EGR-1, but not FASN, in histologically normal tumor adjacent tissues, a result that is in complete agreement with our functional findings in the cell models (see above). The table below lists the Pearson correlations between CD9 and EGR-1, and between CD9 and FASN in the three types of tissues analyzed, i.e. cancerous, histologically normal adjacent, and disease-free. The figure to the right (D) shows the scatter plot for the positive correlation between CD9 and EGR-1 in histologically normal tumor adjacent tissues.

Pearson's Correlations	CD9 / EGR-1	CD9 / FASN
Cancerous	0.065 (p=0.70)	0.494 (p>0.01)
Adjacent	0.727 (p<0.01)	0.528 (p<0.01)
Disease-free	0.439 (p<0.05)	0.572 (p<0.01)



In summary, these data support the hypothesis that exosomes are involved in the etiology of the field effects observed in prostate tissues affected by adenocarcinoma.

Publications

During the period covered by the W81XWH-15-1-0056 grant support, we decided to strengthen the rationale for the choice of markers of prostate field effect with respect to the experimental approaches in Specific Aim 2, where valuable human tissues were utilized, including tissue samples purchased from commercial sources (such as the Cooperative Human Tissue Network), as well as tissue samples from the PI's own repository. Accordingly, our efforts during the first time period covered by grant W81XWH-15-1-0056 included the completion of an extensive association analysis between the four prominent protein markers of prostate field effect, i.e. EGR-1, MIC-1, PDGF-A, and FASN. This is important for example because EGR-1 and FASN are featured centrally in the Specific Aims of W81XWH-15-1-0056. This effort not only revalidated the choice of these markers, but in addition led to the successful submission of a manuscript entitled "*Association and regulation of protein factors of field effect in prostate tissues*" by Kristin N. Gabriel, Anna C. Jones, Kresta S. Antillon, Sara N. Janos, Heidi N. Overton, Shannon M. Jenkins, Emily H. Frisch, Julie PT Nguyen, Kristina A. Trujillo, and Marco Bisoffi. The manuscript was favorably reviewed by the *International Journal of Oncology* (manuscript ID 167557-IJO) and was published (PMID [27634112](https://pubmed.ncbi.nlm.nih.gov/27634112/)). A copy of this publication is provided in the Appendices of this report. Grant support from W81XWH-15-1-0056 is acknowledged in this publication.

We feel that the completion and publication of this manuscript was important for ensuring the successful submission of our next manuscript, which will feature the data relating to the exosomal involvement in the etiology of prostate field effects. Some of the data is shown above. This manuscript is currently being composed.

Building new strategically meaningful alliances

In addition to the already existing collaborations previously established by the PI, during the period covered by the W81XWH-15-1-0056 grant support, we have established new strong and meaningful professional connections. Accordingly, we reached out to leaders in the field of prostate molecular pathology and clinical science. In particular, successful connections with the following individuals and teams were made:

- Dan Mercola, MD/PhD, Department of Pathology, University of California at Irvine (UCI), CA. Dr. Mercola is an internationally known leader in prostate biomarkers, and directs a National Institutes of Health supported tissue repository. Dr. Mercola has invited the PI to present at UCI and has offered access to tissue samples to support his research.
- Veronique Baron, PhD, Vaccine Research Institute of San Diego, CA. Dr. Baron is an expert in EGR-1 biology and has taken an interest in the PI's efforts to elucidate the etiology and role of this transcription factor in prostate field effect.
- Genitourinary disease oriented team (GU-DOT) at the UCI Chao Family Comprehensive Cancer Center (UCICCC) in Orange CA. The GU-DOT is led by a consortium of clinicians and translational researchers. The PI (Marco Bisoffi) has become an Associate Member of the UCICCC and has presented and discussed his research at GU-DOT and at the UCICCC Annual Retreats.

The PI feels that it was important to add expertise, support, and resources to complete the tasks featured in the grant proposal W81XWH-15-1-0056.

Goals not met

We report two aspects, one from each original Specific Aim, that we feel we have not fully met. These are briefly outlined here.

- From Aim 1: The phenotypic effect of prostate cancer exosomes on non-cancerous (normal) human prostate epithelial cells. We will test the effect of exosomes on the metabolic activity, proliferation, and migration of recipient cells.
- From Aim 2: The potential difference between the association of exosomal markers and markers of field effect in tissues harboring unifocal vs. multifocal prostate cancer. We will test this in selected cases of our existing tissue cohort.

We plan to complete these investigations after the official closure of grant W81XWH-15-1-0056.

What opportunities for training and professional development has the project provided?

Grant proposal W81XWH-15-1-0056 provided training to the following individuals:

- Dr. Neda Sadeghiani- Pelar. Dr. Sadeghiani- Pelar joint the research team for a little bit over a 6-months as a postdoctoral fellow. Her contribution in establishing the exosomes isolation techniques were substantial. She will be a co-author on the manuscript currently under composition.
- Undergraduate students (n = 4). The PI conducts research with involvement of up to 8 undergraduate students per semester. Four students were involved in the tasks covered by grant W81XWH-15-1-0056. At least one of the students, Ms. Julie Nguyen, contributed substantially to the results and will thus be featured as a co-author on the manuscript currently under composition.

How were the results disseminated to communities of interest?

The PI maintains a continuous effort to present his research and the supporting agencies, including the DOD PCRP, to members of the scientific and broader community. Two examples of this effort and covered during the support period of grant W81XWH-15-1-0056 are listed below:

- 2015 University of California Irvine (UCI) Chao Family Comprehensive Cancer Center, Genitourinary Disease Oriented Team (GU-DOT), Orange CA: “Prostate Field Cancerization – Molecular Evidence and Clinical Importance”.
- 2016 Osher Lifelong Learning Institute at the California State University Fullerton, Fullerton CA: “Field Cancerization / Field Effect – Thinking Outside The Tumor”.

What do you plan to do during the next reporting period to accomplish the goals?

Nothing to report. This is a final report.

4. Impact

What was the impact on the development of the principal discipline(s) of the project?

The impact of the present research is represented by its responsiveness to the PCRP Overarching Challenges “Develop better tools for early detection of clinically relevant disease”, “Distinguish aggressive from indolent disease in men newly diagnosed with prostate cancer”, and “Tumor and Microenvironment Biology: Understanding prognosis and progression of prostate cancer”. Multifocality is a major contributor to the complexity and inaccuracy of all aspects of prostate cancer clinical assessment and management. It complicates staging and grading because of increased heterogeneity, and can bar focal therapy for patients with low risk disease (defined as Gleason grade ≤ 6 and a PSA of <10 ng/ml), which represent 40-50% of newly diagnosed prostate cancer cases in populations where screening is part of the standard of care. Focal therapy is an organ-sparing therapeutic intervention by different means aimed at avoiding the side effects of radical therapies which can lower the quality of life. It is complementary to active surveillance and is becoming increasingly accepted as part of the effort of developing personalized approaches for prostate cancer patients in the 21st century. Towards this goal, a detailed understanding of the etiology of tumor multifocality is mandatory. It is conceivable that future therapeutic attempts may include early intervention aimed at inhibiting exosome

shedding and distant tumor formation to suppress multifocality. Proven markers and mediators of field effect could also be used for the detection of tissue areas prone to the formation of tumor foci.

Work achieved under the support of grant W81XWH-15-1-0056 has allowed us to initiate a new investigative direction not previously covered in the scientific community. With respect to next steps, we envisage the following: (i) To extend our findings to tissues featuring multifocal tumors and test a possible correlation between exosomal and field effect markers with the extent of tumor multifocality; (ii) to determine the genomic and proteomic effects of tumor exosomes on normal prostate epithelial and stromal cells for the identification of additional markers; (iii) to functionally recapitulate the formation of a field effect by cancer exosomes in animal models of prostate cancer; and finally (iv) to test the validity of exosomal and field effect markers in active/prospective cohorts of patients enrolled in active surveillance.

What was the impact on other disciplines?

Nothing to report.

What was the impact on technology transfer?

Nothing to report.

What was the impact on society beyond science and technology?

As mentioned earlier, the PI maintains a continuous effort to present his research to members of the broader community. One notable example was a presentation in 2016 to the Osher Lifelong Learning Institute at the California State University Fullerton, Fullerton CA entitled “Field Cancerization / Field Effect – Thinking Outside The Tumor”. Such presentations rely heavily on skills of science communication and have the potential to increase the support from the community for translational research, which is of utmost importance for the quest of combatting and eradicating human medical conditions of high societal burden, including prostate cancer. In this particular case, the PI firmly believes that good skills in science communication and the willingness to speak in public will lead to the continuous support of the research orchestrated by the Congressionally Directed Medical Research Programs (CDMRP). The PI also believes that he has successfully contributed to this quest.

5. Changes/Problems

The requested extensions in the time line of grant proposal W81XWH-15-1-0056 have been reported in the previous annual / interim reports. These were based on the necessity to complete a manuscript supporting the continuation of the indicated work, as well as on the PI’s efforts to reach out to leaders in the field for consultation to ensure the validity of scientific direction.

No problems are reported.

6. Products

Publications

The reviewer is referred to the information provided under 3. Accomplishments and Publications on page 5.

Presentations (oral)

- 2015 University of California Irvine (UCI) Department of Pathology, Irvine CA: “Prostate Field Cancerization – Molecular Evidence and Clinical Importance”.
- 2015 University of California Irvine (UCI) Chao Family Comprehensive Cancer Center, Genitourinary Disease Oriented Team (GU-DOT), Orange CA: “Prostate Field Cancerization – Molecular Evidence and Clinical Importance”.
- 2016 Osher Lifelong Learning Institute at the California State University Fullerton, Fullerton CA: “Field Cancerization / Field Effect – Thinking Outside The Tumor”.

Presentations (poster)

- 2015 TriBeta Research Conference in Monterey Bay CA. “Molecular insights into prostate field cancerization”. Frisch E, Bisoffi M.
- 2015 University of California at Irvine (UCI) Chao Family Comprehensive Cancer Center Annual Retreat, Palm Springs CA. “Elucidating molecular pathways of prostate field cancerization: Potential role of EGR-1 as a master regulator”. Gabriel K, Bisoffi M.
- 2016 University of California at Irvine (UCI) Chao Family Comprehensive Cancer Center Annual Retreat, Long Beach CA. “Determining the Role of Exosomes in Prostate Field Cancerization”. Nguyen J, Bisoffi M.
- 2017 TriBeta Pacific District Convention at Las Positas College, Livermore, CA. “Association between cancer exosomes and prostate field cancerization”. Pytak P, Bisoffi M.

7. Participants & Other Collaborating Organizations

What individuals have worked on the project?

The work proposed in grant proposal W81XWH-15-1-0056 was entirely performed at Chapman University, Schmid College of Science and Technology, Chemistry and Biochemistry Program, where the PI has established a new research program. The PI himself was a major participant on the project. In addition, and as outlined under “3. Accomplishments” and “opportunities for training and professional development” on page 6, the following individuals have also participated:

- Dr. Neda Sadeghiani- Pelar. Dr. Sadeghiani- Pelar joined the research team for a little bit over a 6-months as a postdoctoral fellow in 2015. Her contribution in establishing the exosomes isolation techniques were substantial.
- Undergraduate students (n = 4). The PI conducts research with involvement of up to 8 undergraduate students per semester. Four students were involved in the tasks covered by grant W81XWH-15-1-0056. At least one of the students, Ms. Julie Nguyen, contributed substantially to the work.

8. Special Reporting Requirements

None to report.

9. Appendices

The appendix contains a copy of the published manuscript “*Association and regulation of protein factors of field effect in prostate tissues*” by Kristin N. Gabriel, Anna C. Jones, Kresta S. Antillon, Sara N. Janos, Heidi N. Overton, Shannon M. Jenkins, Emily H. Frisch, Julie PT Nguyen, Kristina A. Trujillo, and Marco Bisoffi, published in the International Journal of Oncology (PMID [27634112](https://pubmed.ncbi.nlm.nih.gov/27634112/)). The publication acknowledges support from the W81XWH-15-1-0056 award.

Association and regulation of protein factors of field effect in prostate tissues

KRISTIN N. GABRIEL^{1*}, ANNA C. JONES^{2*}, JULIE P.T. NGUYEN¹,
KRESTA S. ANTILLON², SARA N. JANOS², HEIDI N. OVERTON², SHANNON M. JENKINS²,
EMILY H. FRISCH¹, KRISTINA A. TRUJILLO³ and MARCO BISOFFI^{1,2}

¹Biochemistry and Molecular Biology, Schmid College of Science and Technology, Chapman University, Orange, CA; Departments of ²Biochemistry and Molecular Biology and ³Cell Biology and Physiology, University of New Mexico Health Sciences Center, Albuquerque, NM, USA

Received May 9, 2016; Accepted August 8, 2016

DOI: 10.3892/ijo.2016.3666

Abstract. Field effect or field cancerization denotes the presence of molecular aberrations in structurally intact cells residing in histologically normal tissues adjacent to solid tumors. Currently, the etiology of prostate field-effect formation is unknown and there is a prominent lack of knowledge of the underlying cellular and molecular pathways. We have previously identified an upregulated expression of several protein factors representative of prostate field effect, i.e., early growth response-1 (EGR-1), platelet-derived growth factor-A (PDGF-A), macrophage inhibitory cytokine-1 (MIC-1), and fatty acid synthase (FASN) in tissues at a distance of 1 cm from the visible margin of intracapsule prostate adenocarcinomas. We have hypothesized that the transcription factor EGR-1 could be a key regulator of prostate field-effect formation by controlling the expression of PDGF-A, MIC-1, and FASN. Taking advantage of our extensive quantitative immunofluorescence data specific for EGR-1, PDGF-A, MIC-1, and FASN generated in disease-free, tumor-adjacent, and cancerous human prostate tissues, we chose comprehensive correlation as our major approach to test this hypothesis. Despite the static nature and sample heterogeneity of association studies, we show here that sophisticated data generation, such as by spectral image acquisition, linear unmixing, and digital quantitative imaging, can provide

meaningful indications of molecular regulations in a physiologically relevant *in situ* environment. Our data suggest that EGR-1 acts as a key regulator of prostate field effect through induction of pro-proliferative (PDGF-A and FASN), and suppression of pro-apoptotic (MIC-1) factors. These findings were corroborated by computational promoter analyses and cell transfection experiments in non-cancerous prostate epithelial cells with ectopically induced and suppressed EGR-1 expression. Among several clinical applications, a detailed knowledge of pathways of field effect may lead to the development of targeted intervention strategies preventing progression from pre-malignancy to cancer.

Introduction

Several pre-malignant states of prostate tissues have been previously described to indicate the progression to prostate adenocarcinoma (prostate cancer). Perhaps the most prominent histological deviation from normalcy is prostatic intraepithelial neoplasia (PIN), which can manifest itself as a low- or high-grade form (1). All forms of PIN are characterized by the presence of intraluminal proliferation of the secretory cells of the duct acinar system and abnormal cytological features, including the ratio of nuclear-to-cytoplasmic area, the size of nucleoli, and the chromatin content (2). Another form of pre-malignancy is accepted to be proliferative inflammatory atrophy (PIA), which constitutes a possible link between inflammation and the malignant transformation of prostatic tissues (3). PIA is mainly recognized in low-magnification microscopy by a distinct hyperchromatic appearance of glandular components and variable acinar calibers, and a marked presence of inflammatory cells (4). Of note, both PIN and PIA are histologically evident lesions that are identifiable by trained surgical pathologists. However, it is reasonable to postulate that cell morphological changes leading to histologically abnormal appearances of prostate glands are preceded by molecular alterations that occur in complete absence of any cytological or histological change. This definition is in complete agreement with the concept of 'field effect' or 'field cancerization', two terms that are used interchangeably in this report to reflect contemporary research efforts. Originally introduced for

Correspondence to: Dr Marco Bisoffi, Biochemistry and Molecular Biology, Schmid College of Science and Technology, Chapman University, 1 University Drive, Orange, CA 92866, USA
E-mail: bisoffi@chapman.edu

*Contributed equally

Abbreviations: EGR-1, early growth response-1; FASN, fatty acid synthase; MIC-1, macrophage inhibitory cytokine-1; PDGF-A, platelet-derived growth factor-A

Key words: prostate cancer, field effect, protein factors

renegade cancer cells outside the margins of squamous oral cell carcinoma (5), the updated definition excludes cellular and histological changes and focuses on molecular aberrations (6). Thus, 'field-cancerized' prostate tissues have been recently characterized by us and others (7-10) by genetic, epigenetic, and biochemical alterations in structurally intact epithelial and stromal cells of histologically normal tissues adjacent to prostate adenocarcinomas.

Along this line, we have recently described four protein factors of prostate field effect. These include the key transcription factor early growth response-1 (EGR-1), the lipogenic enzyme fatty acid synthase (FASN), and the secreted growth factors platelet-derived growth factor-A (PDGF-A) and macrophage inhibitory cytokine-1 (MIC-1) (11-13). Our previous reports focused on emphasizing the similarity of the expressions of these factors between tumor tissues and their adjacent tissue areas, thereby supporting the concept of a field effect. Field effect in the prostate has been recognized to be of potential clinical value (7-10), which ideally necessitates an understanding of its underlying causative functional pathways. Towards this goal, the specific purpose of the present study was to explore a possible regulatory association between the transcription factor EGR-1 and the expression of PDGF-A, MIC-1, and FASN. Our primary focus was the analysis of this potential regulatory network by mining extensive datasets consisting of expression levels of EGR-1, PDGF-A, MIC-1, and FASN, in human prostate tissues. Findings from these analyses were corroborated by ectopic control of EGR-1 and its effect on PDGF-A, MIC-1, and FASN expression in the non-cancerous RWPE-1 human prostate epithelial cell model. Accordingly, our data indicate that the key transcription factor EGR-1 positively regulates PDGF-A and FASN, and negatively regulates MIC-1. These associations provide novel insight into the pathways underlying prostate field effect, which may lead to the development of targeted intervention strategies preventing progression from pre-malignancy to cancer.

Materials and methods

Tissues. The tissue cohort utilized in the present study represents a combination of the cohorts reported in our previous studies on prostate field effect (12,13). These tissues were collected in agreement with all Federal, State, and University laws, from consenting patients undergoing prostatectomy and donating ~100-500 mg of remnant tissue for molecular analyses. Individual cases of de-identified disease-free tissue samples were obtained from the Cooperative Human Tissue Network (CHTN) supported by the National Institutes of Health (NIH; Vanderbilt University, Nashville, TN, USA). All tissues were available as formalin-fixed and paraffin-embedded (FFPE) sections of 5- μ m thickness [processed by the Department of Pathology, University of New Mexico Health Sciences Center (Albuquerque, NM, USA) or provided by CHTN]. The study was approved by the Institutional Review Board of the University of New Mexico Health Sciences Center specifically approved the present study (#05-417). The combined tissue cohort consisted of 14 adenocarcinomas, 16 tumor-adjacent tissues, and 9 disease-free tissues. Twelve tumor-adjacent and tumor tissues were matched; for the missing unmatched tissues, the quality of

data was insufficient for inclusion into the final results. The definition of the term 'tumor-adjacent' in our studies refers to tissue resected at a distance of ~1 cm from the visible tumor margin. The definition of the term 'disease-free' refers to prostate specimens from autopsy cases from individuals who died due to conditions unrelated to cancer. All tissues had been histologically reviewed previously by the surgical pathologist E.G. Fischer (Department of Pathology, University of New Mexico Health Sciences Center), especially to exclude the presence of cryptic cancer cells in the tumor-adjacent prostate tissues (12,13). The mean age of all cases utilized was 56.1 years with a range of 26-79 years. The cancer specimens featured Gleason scores from 6 to 9 and pathological tumor node metastasis (TNM) stages (according to the American Joint Committee on Cancer; <https://cancerstaging.org/Pages/default.aspx>) from T2c to T3b (Table I).

Quantitative immunofluorescence. The generation of quantitative immunofluorescence data was reported in our previous studies on prostate field effect (12,13). These procedures included deparaffinization, antigen retrieval, and immunostaining using specific primary antibodies and Alexa Fluor 633-conjugated secondary antibodies. For reference purposes, we list here the specific reagents, while the experimental details have been described (12,13). The primary antibodies were: anti-EGR-1 mouse monoclonal antibody ab54966 (at 3 μ g/ml); anti-MIC-1 goat polyclonal antibody ab39999 (at 3 μ g/ml) (both from Abcam, Cambridge, MA, USA); anti-PDGF-A rabbit polyclonal antibody sc-7958 (at 3 μ g/ml); and anti-FASN rabbit polyclonal antibody sc20140 (H-300) (at 8 μ g/ml) (both from Santa Cruz Biotechnology, Inc., Santa Cruz, CA, USA). The corresponding control antibodies to ensure target specificity at the same concentrations were: normal mouse IgG (GC270; EMD Millipore, Billerica, MA, USA), normal rabbit IgG (10500C), and normal goat IgG (10200) (both from Invitrogen, Carlsbad, CA, USA). The corresponding secondary antibodies were Alexa Fluor 633-conjugated goat anti-mouse IgG, Alexa Fluor 633-conjugated goat anti-rabbit IgG, and Alexa Fluor-conjugated rabbit anti-goat IgG (A21052, A21070, A21086, respectively; all from Invitrogen). Nuclear counterstaining was performed with 4',6-diamidino-2-phenylindole (DAPI).

Quantitative assessment of fluorescence was by spectral image acquisition and linear unmixing modes of confocal microscopy performed at the University of New Mexico Health Sciences Center, Fluorescence Microscopy Shared Resource Core Facility, as described previously by us (12,13). Of note, control tissue slides with DAPI only, secondary antibody only, as well as unstained tissue were imaged separately to generate specific emission spectra for nuclear staining (DAPI; 405 nm excitation, 433 nm emission), Alexa Fluor (633 nm excitation, 490 nm emission), and background autofluorescence (ditto as per Alexa Fluor), respectively. These spectra were subjected to linear unmixing, a process that was equally applied to all spectral images to ensure the validity of inter-tissue comparisons. Consistent with our previous studies (12,13), quantification was achieved by digital imaging of the spectrally unmixed confocal images using two data acquisition modes. i) Whole-image analysis: the total Alexa Fluor 633

Table I. Demographics and clinical parameters of prostate tissues, and number of images analyzed.^a

Prostate tissues	Age (years)	TNM ^b	Gleason	No. of images analyzed ^c							
				EGR-1	MIC-1	PDGF-A	FASN				
Disease-free (CHTN)											
1	26	Not applicable	Not applicable	3	3	--	3				
2	43	Not applicable	Not applicable	3	3	--	3				
3	46	Not applicable	Not applicable	3	--	3	4				
4	79	Not applicable	Not applicable	3	4	2	--				
5	43	Not applicable	Not applicable	3	3	3	4				
6	55	Not applicable	Not applicable	3	3	2	4				
7	55	Not applicable	Not applicable	3	--	--	4				
8	45	Not applicable	Not applicable	3	--	--	3				
9	n/a ^d	Not applicable	Not applicable	3	--	--	--				
Total				27	16	10	25				
Tumor and adjacent (UNMH/CHTN) ^e											
Prostate tissues	Age (years)	TNM ^b	Gleason	Tumor				Adjacent			
				EGR-1	MIC-1	PDGF-A	FASN	EGR-1	MIC-1	PDGF-A	FASN
1	51	n/a ^d	7 (3+4)	--	3	--	--	--	--	--	--
2	54	T3a	7 (3+4)	--	3	--	--	--	--	--	--
3 (m)	59	T3b	9 (4+5), 6 (3+3)	3	3	3	3	3	3	3	3
4 (m)	63	T3a	6 (4+3)	--	5	2	--	--	3	3	--
5 (m)	69	T2c	7 (4+3)	3	3	6	3	6	3	3	3
6 (m)	68	T3b	8 (5+3)	3	4	3	3	3	3	3	3
7 (m)	55	T2c	8 (3+5)	3	6	9	--	6	6	--	--
8 (m)	57	T3a	7 (4+3)	3	3	3	3	3	3	3	3
9 (m)	55	T2c	8 (3+5)	3	--	3	3	6	--	3	9
10 (m)	54	T2-T3	6 (3+3)	--	--	--	3	6	--	6	6
11	54	T2c	6 (3+3)	--	--	--	--	9	--	5	9
12 (m)	64	T3b	6 (3+3)	3	--	4	--	9	--	4	--
13	62	T2c	6 (3+3)	--	--	--	--	9	9	9	16
14 (m)	62	T3b	7 (4+3)	3	4	3	4	6	5	3	9
15 (m)	44	T2c	6 (3+3)	3	--	3	4	5	--	--	6
16	58	T2c	9 (4+5)	--	--	--	--	9	--	--	10
17	69	T2c	6 (3+3)	--	--	--	--	9	--	--	12
18 (m)	68	T3a	7 (3+4)	3	3	3	4	3	6	--	4
Total				30	37	42	30	92	41	45	93

^aA total of 14 adenocarcinomas (tumor), 16 tumor-adjacent tissues (adjacent), and 9 disease-free tissues were analyzed. In total, 488 images were queried (numbers for each case and marker are indicated). Specimens were collected at the University of New Mexico Hospital (UNMH; Albuquerque, NM, USA) or obtained from the CHTN. ^bTNM pathological stage was assigned using criteria published by the American Joint Committee on Cancer (<https://cancerstaging.org/Pages/default.aspx>). ^c--, indicates no available images of sufficient quality. ^dn/a, not available. ^e(m), indicates tumors that were matched with their corresponding adjacent tissues. CHTN, Cooperative Human Tissue Network; TNM, tumor node metastasis; EGR-1, early growth response-1; MIC-1, macrophage inhibitory cytokine-1; PDGF-A, platelet-derived growth factor-A; FASN, fatty acid synthase.

signal was ratio-normalized to the total DAPI signal to account for the number of cells and the cell density per slide, which tends to be different between cancerous and non-cancerous tissues. For EGR-1, the whole-image data acquisition mode

was applied in three settings, i.e., whole-cell (no selection), nuclear selection, and cytoplasmic selection, according to its ability to translocate between the two cell compartments (14). ii) Region of interest (ROI) analysis: three representative ROIs

(defined as areas with robust immunostaining) per slide were chosen and the cumulative signal specific for Alexa Fluor 633 was determined. The ROI acquisition mode was applied to all factors according to their typical expression, i.e., both nuclear and cytoplasmic for EGR-1, extranuclear for MIC-1 and PDGF-A, and cytoplasmic for FASN. The size of ROI was identical from image to image (~80 μm^2 each) and they were chosen by persons blinded to the nature of the tissue (Mrs. Virginia Severns, Ms. Fiona Bisoffi, Ms. Suzanne Jones) to avoid bias (Fig. 1B). All original red signals were converted to yellow for better visibility. In total, 488 images with associated quantitative immunofluorescence data were available for the present analysis (Table I).

Computational transcription factor binding site analysis. Computational searches for a potential transcription factor binding site were performed using the Tfsitescan software of the Molecular Informatics Resource for the Analysis of Gene Expression (MIRAGE) provided by the Institute for Transcriptional Informatics (IFTI; <http://www.ifti.org/cgi-bin/ifti/Tfsitescan.pl>). Genomic sequences for EGR-1, PDGF-A, MIC-1, and FASN were retrieved from the GRCh38 primary assembly of the gene database available at the National Center for Biotechnology Information (NCBI; <http://www.ncbi.nlm.nih.gov/>). The specific reference sequences and locations were: NC_000005.10, *Homo sapiens* chromosome 5, location 138,465,492-138,469,315 for EGR-1; NC_000019.10, *Homo sapiens* chromosome 19, location 18,386,158-18,389,176 for MIC-1; NC_000007.14, *Homo sapiens* chromosome 7, location 497,258-520,123 for PDGF-A; and NC_000017.11, *Homo sapiens* chromosome 17, location 82,078,338-82,098,230 for FASN. The genomic sequences were subjected to searches for the EGR-1 recognition sequence [GCG(G/T)GGCG] (15).

Cell culture and transfections. Non-cancerous RWPE-1 human prostate epithelial cells were purchased from the American Type Culture Collection (Manassas, VA, USA) and cultured in serum-free keratinocyte basal medium containing 4,500 mg/l glucose, 0.05 mg/ml bovine pituitary extract and 5 ng/ml recombinant epidermal growth factor (Invitrogen). Cells were maintained at 37°C in a humidified 5% CO₂ atmosphere. Trypsin-EDTA at 0.25% was used to detach the cells for splitting and reculturing. pcDNA3.1 control and pcDNA3.1/EGR-1 plasmids were a kind gift of Dr W. Xiao (University of Science and Technology of China, Hefei, China). pLKO.1 control and pLKO.1/EGR-1 shRNA plasmids were from Sigma (St. Louis, MO, USA). Plasmids were propagated in *E. coli* strain JM109 grown in LB broth containing 100 $\mu\text{g}/\text{ml}$ ampicillin and purified using spin column chromatography (Qiagen, Inc., Valencia, CA, USA). Transfections were performed with 1 μg plasmid DNA in 24-well plates containing 150,000 cells/well using Lipofectamine 2000 reagent (Invitrogen) for 48 h. Our transfection protocol yields reproducible transfection rates of 45±5% for pairs of empty control and cDNA-carrying plasmids (fluorescence-based assay, not shown). Cells were snap-frozen in liquid nitrogen to preserve RNA integrity and stored short-term at -80°C.

Quantitative reverse transcriptase-polymerase chain reaction (qRT-PCR) and western blotting. RNA was isolated using

spin column chromatography (Qiagen, Inc.). A total of 1-3 μg of RNA was transcribed to cDNA using random decamers of the Retroscript™ RT Kit (Ambion/Life Technologies, Carlsbad, CA, USA). mRNA expression was quantitated in a CFX Connect Real-Time PCR Detection System from Bio-Rad (Hercules, CA, USA) using the SYBR-Green PCR Master Mix and SYBR-Green RT-PCR Reagents Kit (Applied Biosystems/Life Technologies, Carlsbad, CA, USA) in 25- μl reactions, using 100 ng of template cDNA and a final primer concentration of 900 nM. The cycling parameters were 95°C for 5 min followed by 45 cycles of 94°C for 15 sec, and 51-58°C for 1 min. Primers were designed using Primer Express software (Invitrogen) and synthesized by Integrated DNA Technologies (Coralville, IA, USA). The following primer sequences (5'→3') were used: EGR-1 forward, GAGCAG CCCTACGAGCAC and reverse, AGCGGCCAGTATAGG TGATG; MIC-1 forward, CTACAATCCCATGGTGCTCAT and reverse, TCATATGCAGTGGCAGTCTTT; PDGF-A forward, CGTAGGGAGTGAGGATTCTTT and reverse, GCTTCCTCGATGCTTCTCTT; FASN forward, AGAACT TGCAGGAGTTCTGGGACA and reverse, TCCGAAGAA GGAGGCATCAAACCT; TATA-binding protein (TBP) forward, CACGAACCACGGCACTGATT and reverse, TTT TCTTGCTGCCAGTCTGGAC. qRT-PCR reactions were performed in triplicate. Relative expression levels were determined by the $\Delta\Delta\text{Ct}$ method using TBP as normalization control after determining that amplification efficiencies were similar to the ones of the control transcripts.

Protein lysates were generated on ice in lysis buffer: 25 mM Tris, 8 mM MgCl₂, 1 mM DTT, 15% glycerol, 1% Triton X-100, protease inhibitor cocktail (Sigma). Insoluble cell material was removed by centrifugation of lysates at 13,000 rpm for 10 min at 4°C. The protein concentration was determined by Bradford assay (Sigma) against a bovine serum albumin (BSA) standard. Total protein (80 μg) was size-separated by sodium dodecyl sulfate-polyacrylamide gel electrophoresis (SDS-PAGE), electro-blotted onto polyvinylidene fluoride (PVDF) membranes, blocked with 5% milk powder in Tris-buffered saline, and probed overnight with anti-EGR-1 and anti- β -actin primary antibodies (sc-189 from Santa Cruz Biotechnology, Inc., Dallas, TX, USA and A1978 from Sigma, respectively). Detection and chemiluminescent visualization (Clarity ECL substrate; Bio-Rad) of EGR-1 and β -actin were performed using host-matched secondary horseradish peroxidase-conjugated antibodies (Sigma). The quantitative signal intensity of bands was determined by densitometry using ImageJ software (<https://imagej.nih.gov/ij/>).

Statistics. EGR-1, PDGF-A, MIC-1, and FASN expression levels were represented by signal intensities (sum pixel count per area) generated by quantitative immunofluorescence analysis (as described above). Straightforward, yet robust statistical methods were applied to the datasets using the Microsoft Excel software package (Microsoft, Redmond, WA, USA). The datasets were inclusive (all available informative images), for matched cases only, or separated by the means. These approaches are indicated in the 'Results' section.

Correlations between the expressions of EGR-1 and PDGF-A, MIC-1, and FASN were analyzed by several statistical methods. To control for small sample size and a distribution

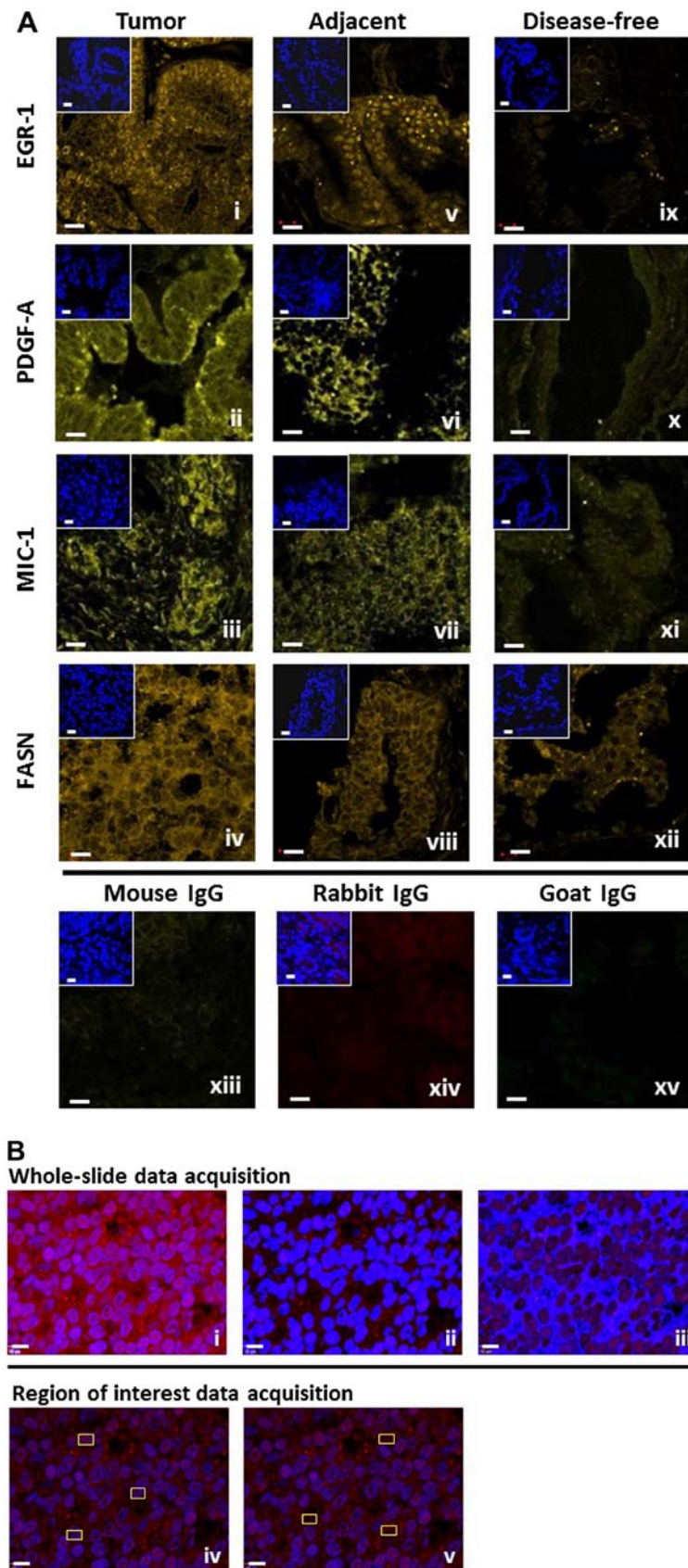


Figure 1. (A) Representative detection of EGR-1, PDGF-A, MIC-1, and FASN by immunofluorescence in tumor (panels i-iv), tumor-adjacent (panels v-viii), and disease-free (panels ix-xii) human prostate tissues. Unspecific IgG of mouse, rabbit, and goat origin were tested for absence of staining (panels xiii-xv). Images represent Alexa Fluor 633 immunostaining (yellow signals); the smaller insets represent corresponding nuclear staining by DAPI (blue); white bars, 10 μ m. (B) Schematic representation of the whole-image (top) and ROI (bottom) quantitative acquisition modes for EGR-1 fluorescence intensity. Whole-image data acquisition includes three different settings as defined by DAPI staining, whole-cell/no selection (panel i), nuclear (panel ii), and cytoplasmic (panel iii), as indicated by the bright blue shading. ROI data acquisition includes nuclear (panel iv) and extranuclear/cytoplasmic (panel v), as indicated by the areas designated by the randomly placed yellow rectangle frames ($\sim 80 \mu\text{m}^2$); white bars, 10 μ m. EGR-1, early growth response-1; PDGF-A, platelet-derived growth factor-A; MIC-1, macrophage inhibitory cytokine-1; FASN, fatty acid synthase; ROI, region of interest.

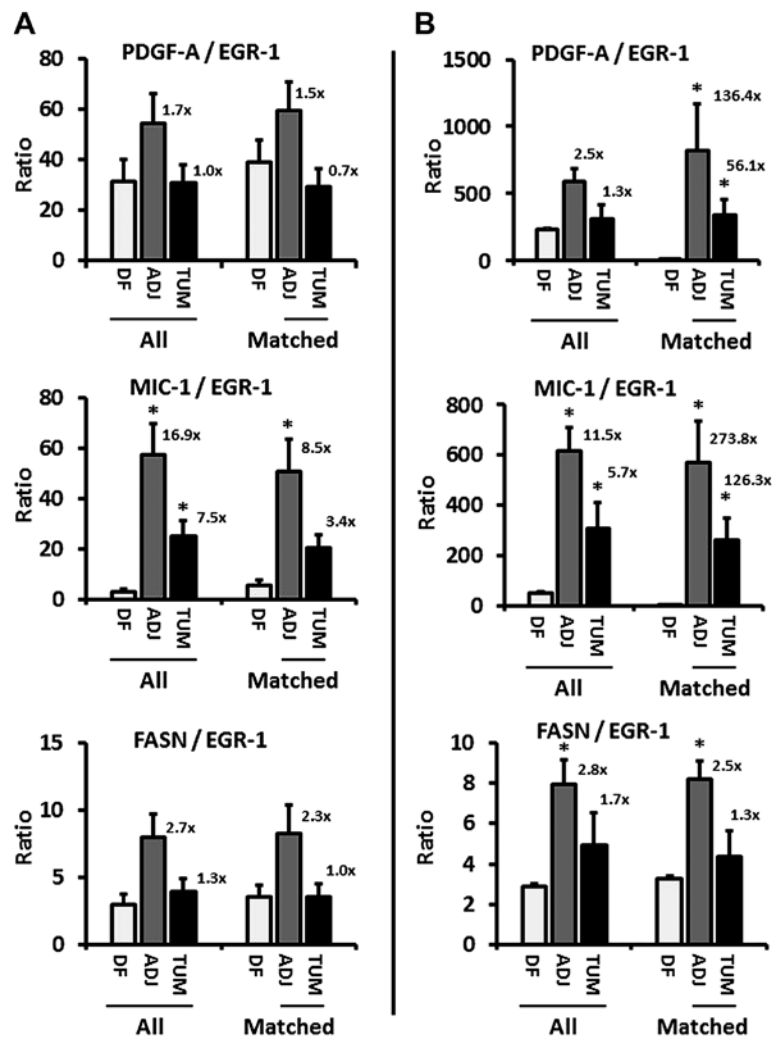


Figure 2. (A and B) Ratios of PDGF-A, MIC-1, and FASN to EGR-1 expression (combined whole-cell, nuclear, cytoplasmic) in disease-free (DF), tumor-adjacent (ADJ), and tumor (TUM) tissues using images from all (left three bars) and matched only (right three bars) cases, acquired by the whole-image and the ROI mode, respectively. The bars represent average ratios + standard errors. The numbers by the bars represent the fold change in ADJ and TUM compared to DF tissues. *Statistical significance compared to DF tissues ($p \leq 0.05$). PDGF-A, platelet-derived growth factor-A; MIC-1, macrophage inhibitory cytokine-1; FASN, fatty acid synthase; EGR-1, early growth response-1; ROI, region of interest.

with infinite variance due to tissue heterogeneity (expressed as coefficient of variation in %; reported in the text of 'Results'), the Wilcoxon rank-sum test (as opposed to the Student's *t*-test) was used for pairs of datasets (reported in the text of 'Results'). The single factor analysis of variance (ANOVA) was applied for comparisons of multiple datasets with unequal variances. Statistical significance for the change of ratios of PDGF-A, MIC-1, or FASN to EGR-1 in tumor-adjacent and tumor tissues as compared to disease-free tissues was determined by the two-tailed Student's *t*-test (statistical significance defined as $p \leq 0.05$; Fig. 2A and B). The datasets were further mined for potential associations between factors by determining the Pearson's correlation coefficient (*r*). The significance for these observations was determined by first calculating the *t*-value of the correlation using the equation $t = r/\text{SQRT}[(1 - r^2)/(n-2)]$, where *r* is the correlation coefficient, *n* is the number of samples, and *n*-2 is the degree of freedom. The *t*-value was then used to determine the significance of *r* by the two-tailed Student's *t*-distribution (TDIST; statistical significance defined as $p \leq 0.05$; reported in the text, but not shown). Statistical significance for the change of ratios of positive to negative

Pearson's correlations of PDGF-A, MIC-1, and FASN to EGR-1 in tumor-adjacent and tumor tissues as compared to disease-free tissues was determined by the *F*-test with $p \leq 0.05$ considered to be significant (Fig. 3B and D).

Results

Immunofluorescence detection of EGR-1, PDGF-A, MIC-1, and FASN in human prostate tissues. We previously reported on the extent of the individual expression of EGR-1, PDGF-A, MIC-1, and FASN to support the concept of field effect in histologically normal prostate tissues adjacent to histologically overt adenocarcinomas, as compared to disease-free tissues (12,13). To begin unraveling the functional pathways of field effect in prostate tissues, here we analyzed the potential association between these markers of field effect in human prostate tissues of different histology. For this analysis, a total of 488 digitized images from 39 individual human prostate tissue samples was available for a comprehensive analysis (Table I). The images indicate the specific detection of EGR-1, PDGF-A, MIC-1, and FASN by immunofluorescence which was quantified

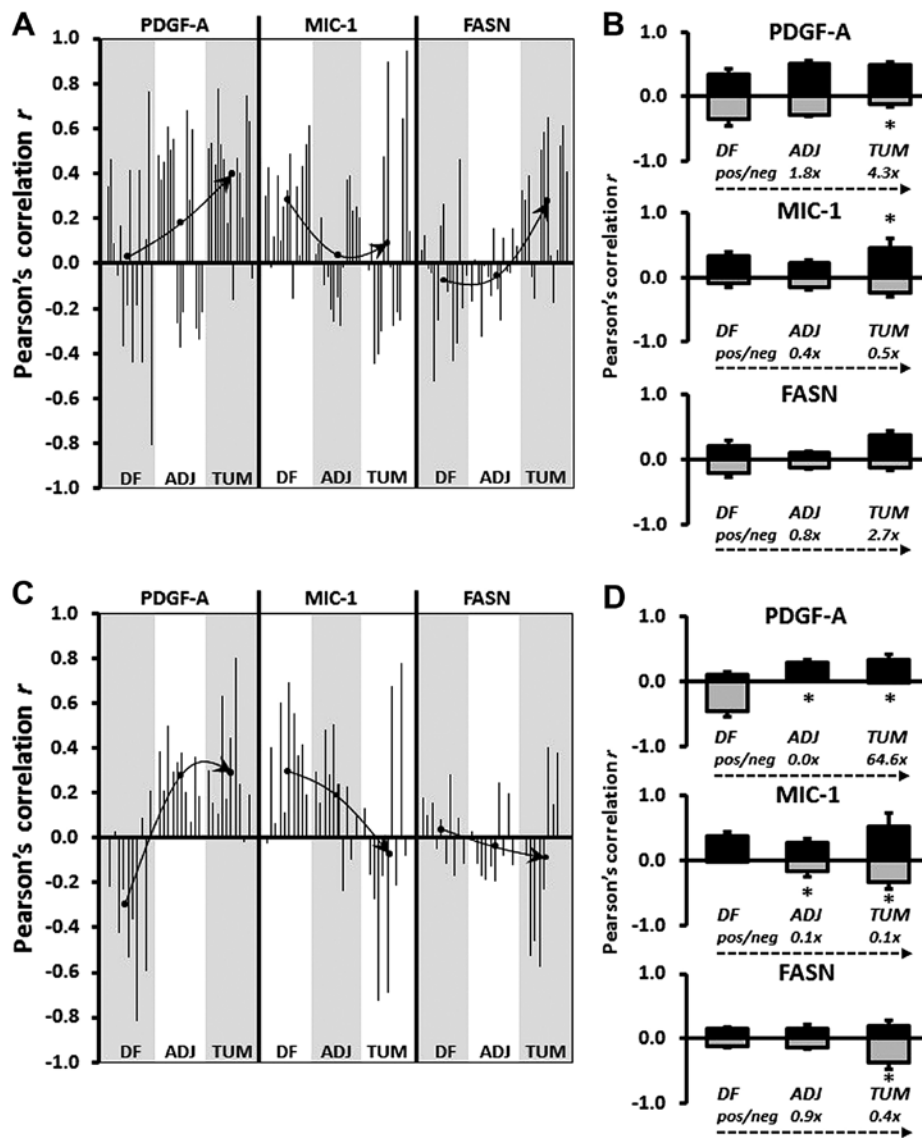


Figure 3. (A and C) Graphical representation of Pearson's correlation (r) between EGR-1 and PDGF-A, MIC-1, and FASN using data from digitized images acquired by the whole-image and the ROI mode, respectively. Within each type of tissue, disease-free (DF), tumor-adjacent (ADJ), and tumor (TUM), correlations were determined for all matched, and for EGR-1 above or below the median with the corresponding median-divided datasets of PDGF-A, MIC-1, and FASN. (A) Datasets consist of whole-cell, nuclear, and cytoplasmic EGR-1 measurements (a total of 15 correlations per factor). (B) Datasets consist of nuclear and cytoplasmic EGR-1 measurements (a total of 12 correlations per factor). Arrows depict the change of regulation by linking the mean Pearson's correlations (black dots) in the different types of tissues. (B and D) Average positive (pos; black bars) and negative (neg; grey bars) Pearson's correlations between EGR-1 and PDGF-A, MIC-1, and FASN in DF, ADJ, and TUM tissues acquired by the whole-image and the ROI mode, respectively. The bars represent average ratios + standard errors. The numbers represent the fold change in the ratio of positive/negative r in ADJ and TUM compared to DF tissues. *Statistical significance compared to DF tissues ($p \leq 0.05$). EGR-1, early growth response-1; PDGF-A, platelet-derived growth factor-A; MIC-1, macrophage inhibitory cytokine-1; FASN, fatty acid synthase; ROI, region of interest.

computationally (12,13). Representative images are shown in Fig. 1A. In general, the expressions of EGR-1, PDGF-A, MIC-1, and FASN were highest in tumor and lowest or absent in disease-free tissues (Fig. 1A, panels i-iv and ix-xii, respectively). Furthermore, tumor-adjacent tissues tended to display elevated expression of all factors (Fig. 1A, panels v-viii). The specificity of detection was corroborated by the absent staining with isotype-specific control antibodies (Fig. 1A, panels xiii-xv).

Quantification and association analyses of EGR-1, PDGF-A, MIC-1, and FASN expressions in human prostate tissues. We have previously developed sensitive quantification methods

for signals generated by immunofluorescence in human prostate tissues [(12,13) and the 'Materials and methods']. These methods include whole-image and ROI data acquisition modalities for all investigated factors (in the 'Materials and methods'). Furthermore, in line with the aim of this study to be as comprehensive as possible with respect to associative analyses, EGR-1 expression was measured using three specific settings for cell compartmentalization: whole-cell, as well as nuclear and cytoplasmic separately. This is supported by an elegant study by Mora *et al* (14) who showed that EGR-1 can shuttle between these locations depending on cellular type and context. These different types of data acquisition are shown in Fig. 1B.

While our previous reports compared the level of expression for EGR-1, PDGF-A, MIC-1, and FASN in disease-free, tumor-adjacent, and tumor tissues, thereby supporting the concept of field effect (12,13), the primary objective of the present study was to explore a potential relationship between these factors and to determine whether that relationship changes in different types of tissues. As expected, and typical for human tissue studies, both the whole-image and the ROI data acquisition modes resulted in substantial heterogeneity with respect to variation of expression of all factors in disease-free, tumor-adjacent, and tumor tissues. The coefficient of variations ranged from 4.7 to 39.0% in the whole-image and from 3.9 to 31.1% in the ROI measurements.

Quantified expression data were comprehensively analyzed for similarities, discrepancies, and associations using straightforward, yet robust statistical methods. Of note, because of the expected inter- and intra-tissue heterogeneity, the identification of outliers was not meaningful and we adopted an inclusive approach in which we did not exclude any data points. In addition, due to different antibody affinities for their targets, we determined that comparisons of the mean, variance, and distribution of expression data between factors would not be good indicators of a causative regulatory role of EGR-1 for the other factors. In fact, group analysis by ANOVA indicated that all expression patterns in all types of tissues were distinct from each other ($p < 0.001$), and individual comparisons by Wilcoxon rank-sum test were non-informative with respect to the distinction between induction and repression ($p \leq 0.05$) or coupled expression ($p > 0.05$). Consequently, we chose to analyze the change of the ratio of either PDGF-A, MIC-1, or FASN to EGR-1 in disease-free compared to tumor-adjacent and tumor tissues. Based on our previous results showing that prostate tissues adjacent to adenocarcinomas feature a field effect compared to disease-free tissues (12,13), such a change in ratio would suggest a potential regulatory role of EGR-1 in agreement with its proven upregulation during tumorigenesis and cancer progression (16). Accordingly, EGR-1 expression determined by both the whole-image and ROI acquisition modes in all available tissues revealed an increase of all factors-to-EGR-1 ratios, up to 2.5-fold for PDGF-A, 16.9-fold for MIC-1, and 2.8-fold for FASN (Fig. 2A and B, left bar graphs). Similarly, when analyzed for matched adjacent and tumor tissues only (derived from the same patients, respectively), the ratio of the other factors to EGR-1 in both acquisition modes markedly increased, up to 136.4-fold for PDGF-A, 273.8-fold for MIC-1, and 2.5-fold for FASN (Fig. 2A and B, right bar graphs). While this analysis does not reveal the direction of regulation (positive or negative), the changes do indicate a regulatory function of EGR-1 for PDGF-A, MIC-1, and to a lesser extent for FASN.

The changes in the expression ratio of PDGF-A, MIC-1, and to some extent FASN, prompted us to refine our determination of a potential regulatory effect of EGR-1 on these factors by using Pearson's correlation analysis, which is independent of differences in antibody affinities for the different factors. By definition, this approach included tissues from matched cases only. To refine our analysis, we also separated all expression data by the median and determined the correlation between expression levels above and below median values. Similar to the ratio analysis presented in Fig. 2, we attempted to corroborate possible regulatory effects of EGR-1

for PDGF-A, MIC-1, and FASN expressions by comparing Pearson's correlations between different types of tissues, i.e., disease-free, tumor-adjacent, and tumor tissues. Fig. 3A and C shows a graphical representation of all possible correlations between whole-cell, nuclear, and cytoplasmic EGR-1 and PDGF-A, MIC-1, and FASN expression in disease-free, tumor-adjacent, and tumor tissues as acquired by whole-image and ROI acquisition mode, respectively. In contrast to group analyses by ANOVA or individual comparisons by Wilcoxon rank-sum test, Pearson's correlation analyses are indicators of positive vs. negative regulation. The significance (average p) of the Pearson's correlation coefficients for the whole-image acquisition mode was 0.16, 0.24, and 0.25 (with 40, 7 and 18% of all coefficients being $p \leq 0.05$) for PDGF-A, MIC-1, and FASN, respectively. For the ROI acquisition mode, the significance (average p) for the corresponding factors was 0.21, 0.21, and 0.25 (with 17, 23 and 7% of all coefficients being $p \leq 0.05$). Visual inspection of the Pearson's correlation analyses in Fig. 3A and C indicates that EGR-1 positively and negatively regulates PDGF-A and MIC-1, respectively, while the results for FASN regulation were less clear due to the contrasting data between the two data acquisition modes. Similar to the ratio analysis presented in Fig. 2, we attempted to corroborate possible regulatory effects of EGR-1 for PDGF-A, MIC-1, and FASN expressions by comparing Pearson's correlations between different types of tissues, i.e., disease-free, tumor-adjacent, and tumor tissues. Given the high tissue heterogeneity, we used an inclusive approach and compared the average of all positive and negative correlations ($r > 0$ or < 0) for each factor in the three types of tissues. This analysis showed a progressive positive and negative regulation of PDGF-A (up to 64.6-fold) and MIC-1 (up to 10-fold), respectively, in tumor-adjacent and tumor tissues compared to disease-free tissues. Again, results for FASN were less clear with contrasting results depending on the data acquisition mode (Fig. 3B and D). These possible regulations were confirmed by visually linking the means of Pearson's correlations in the different types of tissues (Fig. 3A and B).

Computational and cell experimental analysis of EGR-1 regulation of PDGF-A, MIC-1, and FASN. The theoretical potential of the transcription factor EGR-1 to be a regulator of PDGF-A, MIC-1, and FASN expression was determined computationally using Tfsitescan software applied to 1,500 bp upstream and 500 bp downstream of the transcription initiation site on the genomic sequences of PDGF-A, MIC-1, and FASN. Thus, a total of 2,000 bp was screened for the presence of the EGR-1 recognition sequence [GCG(G/T)GGCG] (15). This analysis resulted in the identification of two, one, and four recognition sequences for PDGF-A, MIC-1, and FASN, respectively (Fig. 4A). Regulation of PDGF-A, MIC-1, and FASN expression by EGR-1 was experimentally tested by overexpression and suppression of EGR-1 in transient transfection experiments using the non-cancerous RWPE-1 human prostate epithelial cell model. The immortalized but non-cancerous RWPE-1 cells were chosen because they best represent the tissues analyzed in this study, which are almost exclusively early-stage malignancy and tumor-adjacent, i.e., best reflective of field effect. Transfections with the pcDNA3.1 and the pLKO.1 plasmids typically resulted in 50-100-fold

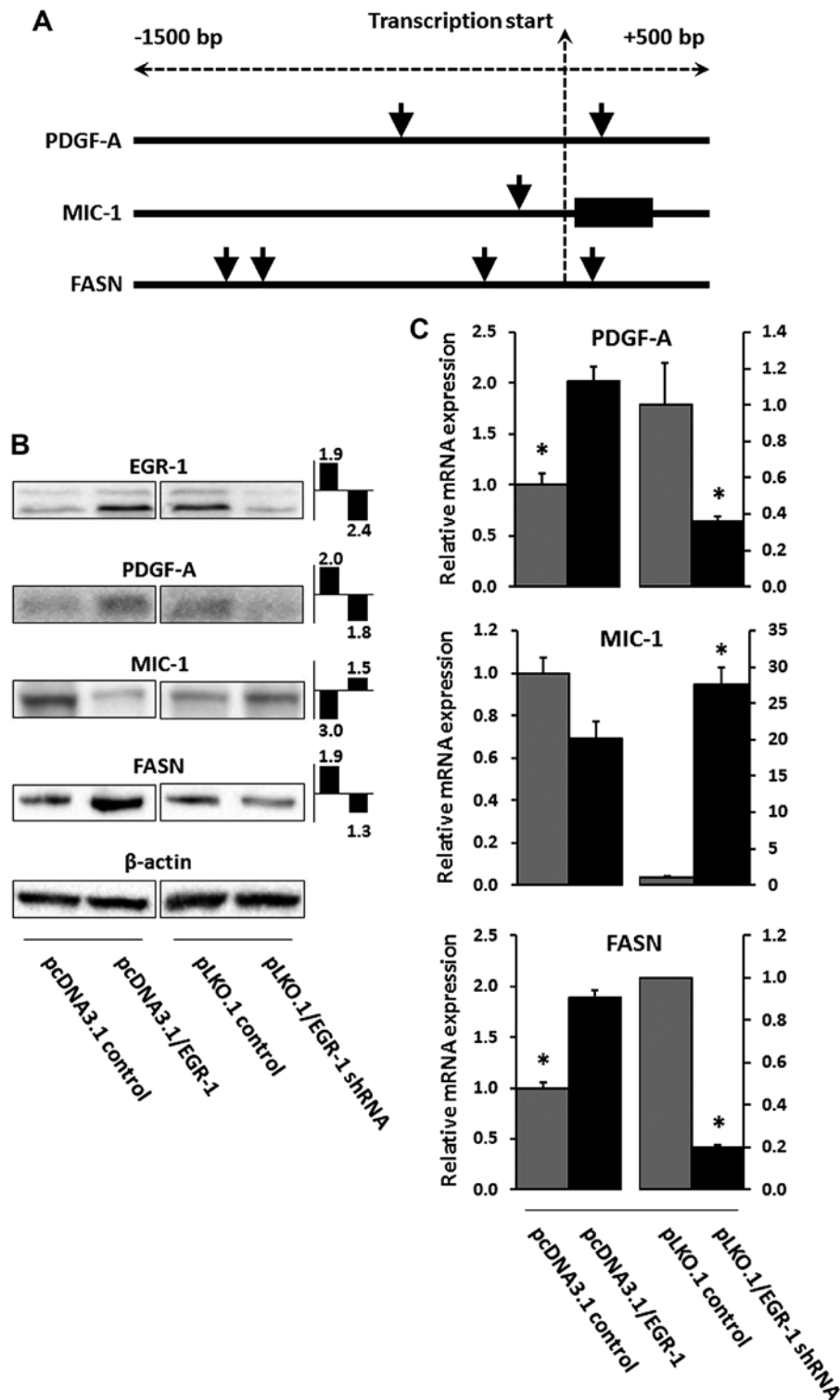


Figure 4. (A) Computational analysis of the EGR-1 recognition sequence [GCG(G/T)GGCG] in the genomic sequence 1,500 bp upstream and 500 bp downstream of the transcription initiation site of PDGF-A, MIC-1, and FASN. Black vertical lines and black rectangular boxes denote genomic sequences and exons, respectively; vertical arrow heads indicate EGR-1 recognition sequences. (B) EGR-1, PDGF-A, MIC-1, and FASN protein expression in RWPE-1 cells transiently transfected with pcDNA3.1/EGR-1 (EGR-1 overexpression) or pLKO.1/EGR-1 shRNA (EGR-1 suppression), and their empty plasmid controls. Double bands in EGR-1 represent post-translational modifications (44). The fold change difference compared to empty plasmid control and determined by densitometry as a ratio with β -actin signal is indicated in the small bar graphs (left bar, EGR-1 overexpression; right bar, EGR-1 suppression). (C) Relative mRNA expression of PDGF-A, MIC-1, and FASN in RWPE-1 cells transiently transfected with pcDNA3.1/EGR-1 (EGR-1 overexpression) or pLKO.1/EGR-1 shRNA (EGR-1 suppression), and their empty plasmid controls. Bars represent averages of triplicates \pm standard deviation; *Statistical significance ($p \leq 0.05$) from pcDNA3.1 and pLKO.1 plasmid vector control, respectively. EGR-1, early growth response-1; PDGF-A, platelet-derived growth factor-A; MIC-1, macrophage inhibitory cytokine-1; FASN, fatty acid synthase.

overexpression and suppression of EGR-1 at the mRNA level (not shown). Modulation of EGR-1 protein expression was

verified by western blotting and resulted in ~ 2 -fold overexpression and suppression. Although the regulatory effects

on PDGF-A, MIC-1, and FASN were rather small, transient EGR-1 overexpression upregulated PDGF-A and FASN protein expression (up to 2-fold) and downregulated MIC-1 protein expression (up to 3-fold), while transient EGR-1 suppression corroborated this effect by upregulating MIC-1 protein expression (~1.5-fold), while downregulating PDGF-A and FASN protein expression (up to 2-fold) (Fig. 4B). These results were accompanied by similar changes at the mRNA level, as measured by qRT-PCR. Accordingly, transient EGR-1 overexpression upregulated PDGF-A and FASN (up to 2-fold) and downregulated MIC-1 (up to 2-fold), while transient EGR-1 suppression corroborated this effect by downregulating PDGF-A and FASN (up to 2.5- and 5-fold, respectively) and by upregulating MIC-1 (up to 10-fold) (Fig. 4C). Overall, these results are in good agreement with the observations made in the tissues.

Discussion

The importance of field effect, or field cancerization, in the prostate has been well-recognized as worthy of being explored in detail for the benefit of developing clinical applications towards a better clinical management of prostate cancer (8-10,17). For example, we have previously argued that prostate field effect could be used to improve the diagnosis of prostate cancer in false-negative biopsies (10). The latter remains an important and continuous challenge in confirmatory diagnosis of prostate adenocarcinoma that has clinical, psychological, and financial implications (18-21). Accordingly, field-cancerized tissue could increase the clinically informative area that can be analyzed microscopically by a surgical pathologist if histology could be combined with immunological techniques. In this scenario, the pathologist would recognize the presence and location of a lesion even in the absence of its visual confirmation thereby avoiding false-negative cells, even after repeated biopsies (22). This possibility has prompted others to term tissues affected by field-effect tumor-indicating normal tissue (TINT) (8). Even in the case of a positive identification of cancer, the extent (number of positive biopsy cores, % of tissue affected) and the grade (Gleason) may indicate a low risk for progression and thus eligibility for active surveillance with frequent testing for serum prostate-specific antigen (PSA), as opposed to prostatectomy (23). It is conceivable that during active surveillance, a recognized field effect could be monitored and queried as an indicator of potential progression (10,24). This would help mitigate the well-known overtreatment of prostate cancer with surgery, which albeit performed with curative intent, may unnecessarily decrease quality of life due to its severe side-effects (25,26). The latter approach could also be amenable to the assessment of pre-surgical neo-adjuvant therapeutic interventions, for which the efficacy could be monitored during active surveillance by established markers and parameters of field effect (10,27). A further potential application of field effect lies in its inclusion in the definition of surgical margins for focal therapy, which seems to be on the rise as a form of less invasive therapy and as more refined interventions have developed (10,28,29). As such, the presence of a field effect at the margin may be indicative of elevated risk for progression or of the extent of tumor multifocality within the prostate (10,30). Of note, the

common assumption underlying the aforementioned potential applications of prostate field effect is that a field exists as a consequence of the presence of a lesion. However, it is also conceivable that field effect precedes tumor formation and represents a truly pre-malignant status evident at the molecular level but in absence of any histological change. In fact, the latter view is widely accepted (8-10,17) and defines field-cancerized prostate tissues as a temporal record of tumorigenesis. As such, it is a source for early biomarkers and potential targets for preventative strategies (8,10).

Pertinent to all applications of field effect is the knowledge of the molecular markers and pathways that are characteristic for it. We and others have previously compiled lists of molecular markers reported in the scientific literature (7-10), but for most of these factors the etiology remains unknown. For markers of field effect to be of best use, either as indicators or as targets, it is important to begin identifying distinct cellular and molecular events and pathways that underlie the formation of a field. Towards this goal, in this report we have established a link between four protein factors of prostate field effect, which were originally identified individually or deduced from the literature. We had identified the key transcription factor EGR-1, the divergent member of the transforming growth factor- β (TGF- β) MIC-1, and the lipogenic oncogene FASN as being elevated in prostate tissues 1 cm from the visible tumor margin (11). While our original study was microarray-based and thus RNA-specific, we subsequently confirmed EGR-1, MIC-1, FASN, and PDGF-A protein upregulation in field-cancerized human prostate tissues (12,13).

EGR-1 is a central regulator of many molecular pathways and acts divergently according to the cell context (31). While in other types of tissues, it may function primarily as a tumor suppressor, it ultimately assumes, with some ambiguity, a tumor-promoting role in prostate cancer development and progression (16,32,33). The role of the secreted factor PDGF-A in prostate cancer is well-established. It is one of four isoforms that binds as a dimer to the tyrosine kinase receptors PDGFR α and β . PDGF-A stimulates growth, survival, and motility of various cell types and when hyperactivated, promotes prostate cancer development and progression through paracrine and autocrine actions (34,35). Equally established in prostate cancer development and progression is FASN, which has been termed a metabolic oncogene and is the target of ongoing efforts to develop specific inhibitors of its lipogenic activity promoting tumor cell proliferation through lipid biosynthesis and post-translational protein modification (36,37). The role of MIC-1 is less clear and is reported as both a cancer promoter and suppressor (38,39). Originally discovered in macrophages (40), it may promote a pro-tumorigenic environment when secreted by prostate cancer cells by suppressing the anticancer activity of immune cells (41).

It is conceivable that the concerted actions of MIC-1, PDGF-A, and FASN can lead to the formation of molecularly altered fields through autocrine stimulation of hyperproliferative cell foci prone to further genetic and biochemical change towards transformation, which is congruent with the definition of a pre-malignant field effect. However, the possibility of cross-regulatory influences of these actions remain unknown. Since EGR-1 is a pleiotropic transcription factor, we hypothesized that it could regulate MIC-1, PDGF-A, and FASN.

The present study aimed at testing this possibility through comprehensive association analyses using quantitative immunofluorescence expression data generated in human prostate tissues. EGR-1 has been previously shown to induce many target genes, including PDGF-A in the LAPC4 cell model of prostate cancer after ectopic overexpression of EGR-1 (42). Similarly, MIC-1 seems to be positively regulated by EGR-1 in the LNCaP prostate cancer cell model (43). In contrast, there is a lack of information for a potential regulatory function of EGR-1 for FASN in prostate cells or tissues, although our computational analysis of genomic DNA up- and downstream of the transcription initiation site indicates multiple EGR-1 recognition sequences. Our own ectopic EGR-1 overexpression and suppression data in RWPE-1 cells confirms a positive regulation of PDGF-A, but resulted in a negative regulation of MIC-1. An obvious reason for this discrepancy is that RWPE-1 represents a non-cancerous pre-malignant, as opposed to an advanced cancer cell model, such as LNCaP (43). At the experimental level, the use of reporter constructs for MIC-1 activity (43) vs. qRT-PCR using specific primers may also have contributed to differences in the result. More importantly however, our *in vitro* findings are supported by our extensive *in situ* association studies in human tissues which are based on factor correlations and their changes from disease-free to tumor-adjacent to histologically abnormal tissues, thereby confirming the presence of a field effect. In fact, using two data acquisition modes our data show a positive association between EGR-1 and both PDGF-A and FASN, which in turn support a positive regulation. In contrast, our results suggest a negative regulation of MIC-1 by EGR-1, which seemingly contradicts our observation that both are upregulated in tumor-adjacent and cancerous prostate tissues when compared to disease-free controls (12). While the latter justifies the inclusion of MIC-1 in the present study, this discrepancy indicates a more complex regulatory network and warrants further investigations using functional approaches in systems that reflect the complexity of human tissues.

In summary, three principal conclusions can be drawn from our findings. First, immunohistochemistry and immunofluorescence are techniques usually employed towards qualitative assessment of protein expression and localization in cells and tissues in a static manner. However, we show here that using sophisticated quantitation methods, such as spectral image acquisition, linear unmixing, and digital imaging developed in our previous reports (12,13), can deliver meaningful indications of molecular associations in a physiologically relevant *in situ* environment, even in the presence of high heterogeneity. A related issue is the use of ROIs in quantitation. ROIs are often used to compensate for inequalities of cell composition. Although our data show good congruency between the whole-image and ROI approaches for the most part, it also cautions for care with respect to the number of ROIs and their random and blinded placement. Second, our study prompts for caution when comparing molecular association data generated in cell models with data stemming from tissues. Although it can be argued that tissue studies are static and compromised by sample heterogeneity, they can provide meaningful indications of molecular regulations when coupled with sophisticated data acquisition. Also, tissues are physiologically relevant, reflect better the complexity of cellular and

molecular pathways influenced by the environment, and can guide confirmatory studies in cell models. Third, we propose EGR-1 to be a key regulator of prostate field effect through induction of pro-proliferative and pro-metabolic (PDGF-A and FASN, respectively) and suppression of pro-apoptotic (MIC-1) factors. This is supported in particular by our comparative data between disease-free and tumor-adjacent tissues (field effect). Admittedly, while the positive regulation of PDGF-A and FASN by EGR-1 can be easily acknowledged, its regulatory function for MIC-1 seems less clear due to its concomitant upregulation in tumor-adjacent tissues (13). However, it is important to note that these findings are not in disagreement, as MIC-1 regulation has been discussed to be complex (38,39). This may be reflected in a complex *in situ* environment, such as tissues, where many other factors may also exert their regulatory effect. Future studies are warranted to test the exact mechanisms of direct and/or indirect regulation under physiological conditions, such as in animal models. Because it is widely accepted that field effect represents a pre-malignant state, such knowledge may help develop targeted intervention strategies preventing progression to cancer.

Acknowledgements

We thank the following individuals at the New Mexico Health Sciences Center, Department of Pathology and Hospital: Trisha Fleet for procuring prostate tissues through patient consent; Myra Zucker, Cathy Martinez, and Kari Rigg for skillfully preparing prostate tissue sections; the surgical pathologist Dr E.G. Fischer for the histological review of all prostate tissues utilized in this study. We acknowledge Kerry Wiles from the CHTN-Western Division at Vanderbilt University Medical Center (Nashville, TN, USA) for the successful procurement of prostate tissues and annotated reports. We are grateful to Genevieve Phillips and Dr Rebecca Lee from the University of New Mexico and Cancer Center, Fluorescence Microscopy Shared Resource for excellence assistance and technical input for generating the images by spectral imaging and linear unmixing. We thank Ms. Virginia Severns, Ms. Fiona Bisoffi, and Ms. Suzanne Jones for the unbiased placing of the ROI boxes for signal quantitation in the tissue images. The departmental offices and staff of the University of New Mexico, Department of Biochemistry and Molecular Biology, Office of Medical Student Affairs, and the Schmid College of Science and Technology, Chapman University are acknowledged for administrative support. This study was supported by NIH grant RR0164880, NIH grant R03CA136030-02, Prostate Cancer Research Program grant W81XWH-15-1-0056 from the Department of Defense (to Dr M. Bisoffi), University of New Mexico Cancer Center Support grant NIH/NCI P30CA118110, grants from the Chapman University Office of Undergraduate Research (to Miss K. Gabriel and Miss E. Frisch), and a generous gift from Melinda and Edward Subia of Orange County, CA, USA.

References

1. Epstein JI: Mimickers of prostatic intraepithelial neoplasia. *Int J Surg Pathol* 18 (Suppl): 142S-148S, 2010.

2. Montironi R, Mazzucchelli R, Algaba F and Lopez-Beltran A: Morphological identification of the patterns of prostatic intraepithelial neoplasia and their importance. *J Clin Pathol* 53: 655-665, 2000.
3. De Marzo AM, Platz EA, Sutcliffe S, Xu J, Grönberg H, Drake CG, Nakai Y, Isaacs WB and Nelson WG: Inflammation in prostate carcinogenesis. *Nat Rev Cancer* 7: 256-269, 2007.
4. De Marzo AM, Marchi VL, Epstein JI and Nelson WG: Proliferative inflammatory atrophy of the prostate: Implications for prostatic carcinogenesis. *Am J Pathol* 155: 1985-1992, 1999.
5. Slaughter DP, Southwick HW and Smejkal W: Field cancerization in oral stratified squamous epithelium; clinical implications of multicentric origin. *Cancer* 6: 963-968, 1953.
6. Braakhuis BJ, Tabor MP, Kummer JA, Leemans CR and Brakenhoff RH: A genetic explanation of Slaughter's concept of field cancerization: Evidence and clinical implications. *Cancer Res* 63: 1727-1730, 2003.
7. Dakubo GD, Jakupciak JP, Birch-Machin MA and Parr RL: Clinical implications and utility of field cancerization. *Cancer Cell Int* 7: 2, 2007.
8. Halin S, Hammarsten P, Adamo H, Wikström P and Bergh A: Tumor indicating normal tissue could be a new source of diagnostic and prognostic markers for prostate cancer. *Expert Opin Med Diagn* 5: 37-47, 2011.
9. Nonn L, Ananthanarayanan V and Gann PH: Evidence for field cancerization of the prostate. *Prostate* 69: 1470-1479, 2009.
10. Trujillo KA, Jones AC, Griffith JK and Bisoffi M: Markers of field cancerization: Proposed clinical applications in prostate biopsies. *Prostate Cancer* 2012: 302894, 2012.
11. Haaland CM, Heaphy CM, Butler KS, Fischer EG, Griffith JK and Bisoffi M: Differential gene expression in tumor adjacent histologically normal prostatic tissue indicates field cancerization. *Int J Oncol* 35: 537-546, 2009.
12. Jones AC, Antillon KS, Jenkins SM, Janos SN, Overton HN, Shoshan DS, Fischer EG, Trujillo KA and Bisoffi M: Prostate field cancerization: Deregulated expression of macrophage inhibitory cytokine 1 (MIC-1) and platelet derived growth factor A (PDGF-A) in tumor adjacent tissue. *PLoS One* 10: e0119314, 2015.
13. Jones AC, Trujillo KA, Phillips GK, Fleet TM, Murton JK, Severns V, Shah SK, Davis MS, Smith AY, Griffith JK, *et al*: Early growth response 1 and fatty acid synthase expression is altered in tumor adjacent prostate tissue and indicates field cancerization. *Prostate* 72: 1159-1170, 2012.
14. Mora GR, Olivier KR, Chevillat JC, Mitchell RF Jr, Lingle WL and Tindall DJ: The cytoskeleton differentially localizes the early growth response gene-1 protein in cancer and benign cells of the prostate. *Mol Cancer Res* 2: 115-128, 2004.
15. Pagel JI and Deindl E: Disease progression mediated by *egr-1* associated signaling in response to oxidative stress. *Int J Mol Sci* 13: 13104-13117, 2012.
16. Gitenay D and Baron VT: Is EGR1 a potential target for prostate cancer therapy? *Future Oncol* 5: 993-1003, 2009.
17. Walia G, Pienta KJ, Simons JW and Soule HR: The 19th annual Prostate Cancer Foundation scientific retreat. *Cancer Res* 73: 4988-4991, 2013.
18. Delongchamps NB and Haas GP: Saturation biopsies for prostate cancer: Current uses and future prospects. *Nat Rev Urol* 6: 645-652, 2009.
19. Eichler K, Hempel S, Wilby J, Myers L, Bachmann LM and Kleijnen J: Diagnostic value of systematic biopsy methods in the investigation of prostate cancer: A systematic review. *J Urol* 175: 1605-1612, 2006.
20. Presti JC Jr: Prostate biopsy strategies. *Nat Clin Pract Urol* 4: 505-511, 2007.
21. Rabbani F, Stroumbakis N, Kava BR, Cookson MS and Fair WR: Incidence and clinical significance of false-negative sextant prostate biopsies. *J Urol* 159: 1247-1250, 1998.
22. Patel AR and Jones JS: Optimal biopsy strategies for the diagnosis and staging of prostate cancer. *Curr Opin Urol* 19: 232-237, 2009.
23. Pomerantz M: Active surveillance: Pathologic and clinical variables associated with outcome. *Surg Pathol Clin* 8: 581-585, 2015.
24. Mazzucchelli R, Galosi AB, Santoni M, Lopez-Beltran A, Scarpelli M, Cheng L and Montironi R: Role of the pathologist in active surveillance for prostate cancer. *Anal Quant Cytopathol Histopathol* 37: 65-68, 2015.
25. Bellardita L, Valdagni R, van den Bergh R, Randsdorp H, Repetto C, Venderbos LD, Lane JA and Korfage IJ: How does active surveillance for prostate cancer affect quality of life? A systematic review. *Eur Urol* 67: 637-645, 2015.
26. Kwon O and Hong S: Active surveillance and surgery in localized prostate cancer. *Minerva Urol Nefrol* 66: 175-187, 2014.
27. Lou DY and Fong L: Neoadjuvant therapy for localized prostate cancer: Examining mechanism of action and efficacy within the tumor. *Urol Oncol* 34: 182-192, 2016.
28. Lindner U, Lawrentschuk N, Schatloff O, Trachtenberg J and Lindner A: Evolution from active surveillance to focal therapy in the management of prostate cancer. *Future Oncol* 7: 775-787, 2011.
29. Marshall S and Taneja S: Focal therapy for prostate cancer: The current status. *Prostate Int* 3: 35-41, 2015.
30. Andreoiu M and Cheng L: Multifocal prostate cancer: Biologic, prognostic, and therapeutic implications. *Hum Pathol* 41: 781-793, 2010.
31. Pagel JI and Deindl E: Early growth response 1 - a transcription factor in the crossfire of signal transduction cascades. *Indian J Biochem Biophys* 48: 226-235, 2011.
32. Adamson E, de Belle I, Mittal S, Wang Y, Hayakawa J, Korkmaz K, O'Hagan D, McClelland M and Mercola D: *Egr1* signaling in prostate cancer. *Cancer Biol Ther* 2: 617-622, 2003.
33. Adamson ED and Mercola D: *Egr1* transcription factor: Multiple roles in prostate tumor cell growth and survival. *Tumour Biol* 23: 93-102, 2002.
34. Heldin CH: Autocrine PDGF stimulation in malignancies. *Ups J Med Sci* 117: 83-91, 2012.
35. Heldin CH: Targeting the PDGF signaling pathway in tumor treatment. *Cell Commun Signal* 11: 97, 2013.
36. Baron A, Migita T, Tang D and Loda M: Fatty acid synthase: A metabolic oncogene in prostate cancer? *J Cell Biochem* 91: 47-53, 2004.
37. Zadra G, Photopoulos C and Loda M: The fat side of prostate cancer. *Biochim Biophys Acta* 1831: 1518-1532, 2013.
38. Husaini Y, Qiu MR, Lockwood GP, Luo XW, Shang P, Kuffner T, Tsai VW, Jiang L, Russell PJ, Brown DA, *et al*: Macrophage inhibitory cytokine-1 (MIC-1/GDF15) slows cancer development but increases metastases in TRAMP prostate cancer prone mice. *PLoS One* 7: e43833, 2012.
39. Vaňhara P, Hampl A, Kozubík A and Souček K: Growth/differentiation factor-15: Prostate cancer suppressor or promoter? *Prostate Cancer Prostatic Dis* 15: 320-328, 2012.
40. Bootcov MR, Bauskin AR, Valenzuela SM, Moore AG, Bansal M, He XY, Zhang HP, Donnellan M, Mahler S, Pryor K, *et al*: MIC-1, a novel macrophage inhibitory cytokine, is a divergent member of the TGF-beta superfamily. *Proc Natl Acad Sci USA* 94: 11514-11519, 1997.
41. Karan D, Holzbeierlein J and Thrasher JB: Macrophage inhibitory cytokine-1: Possible bridge molecule of inflammation and prostate cancer. *Cancer Res* 69: 2-5, 2009.
42. Svaren J, Ehrig T, Abdulkadir SA, Ehrengruber MU, Watson MA and Milbrandt J: EGR1 target genes in prostate carcinoma cells identified by microarray analysis. *J Biol Chem* 275: 38524-38531, 2000.
43. Shim M and Eling TE: Protein kinase C-dependent regulation of NAG-1/placental bone morphogenic protein/MIC-1 expression in LNCaP prostate carcinoma cells. *J Biol Chem* 280: 18636-18642, 2005.
44. Mora GR, Olivier KR, Mitchell RF Jr, Jenkins RB and Tindall DJ: Regulation of expression of the early growth response gene-1 (EGR-1) in malignant and benign cells of the prostate. *Prostate* 63: 198-207, 2005.